Liquid flow in pores: Slip, no-slip, or multilayer sticking

Uwe Heinbuch and Johann Fischer
Institut für Thermo- und Fluiddynamik, Ruhr-Universität, D-4630 Bochum 1, West Germany
(Received 3 November 1988)

The Hagen-Poiseuille flow of a Lennard-Jones liquid through a cylindrical pore formed by regularly arranged fixed atoms is studied by molecular-dynamics (MD) simulations. Different flow patterns develop depending on the strength of the wall-fluid interaction, the strength of the gravitational-type driving force, the thermodynamic state, and also on the mechanism of heat dissipation. In spite of the high driving forces necessary in MD it is found that up to two molecular layers may stick at the wall which confirms recent experimental findings.

The problem to be addressed here is the classical question of slip or no-slip of flows at solid boundaries. On a molecular scale there exists a third case which we call multilayer sticking, i.e., that several adsorbed layers are immobilized at the wall. Recent experiments by Chan and Horn[1] showed strong evidence for that case. On the other hand, recent molecular-dynamics (MD) simulations for the Hagen-Poiseuille[2,3] and the Couette[4] flow in pores arrived at different results. Hannon, Lie, and Clementi[2] definitely found slip. Koplik, Banavar, and Willemsen[3] found that their velocity profile vanishes at the wall within the ambiguity of a molecular diameter and from Fig. 2 in that paper a small drift velocity in the first fluid layer can be seen. The results of Davis and co-workers[4] also show a slight relative drift velocity in the first layer, but show an enhanced viscosity up to the second layer as well.

From earlier studies[5-8] we know that the potential between the fluid particles, the wall-fluid potential, the state condition of the fluid, and eventually the geometry also have a strong influence on the structure of a fluid in equilibrium at a solid. In simulating flow processes we experienced that the strength of the driving force, as well as the mechanism of dissipating the energy, play an important role. Hence, one must be careful in deciding whether a certain finding from MD simulations is due to physically realistic assumptions; presently, the driving forces are always artificially high.

The slip behavior found in Ref. 2 seems to be a direct consequence of the thermal-wall boundary condition which corresponds to the mathematical model of diffuse reflection in the kinetic theory of gases. The physically more realistic boundary is that used in Ref. 3, where the fluid is confined by fixed atoms on a fcc lattice. One problem with the procedure used in Ref. 3, however, is that a weak wall-fluid interaction combined with a strong driving force was used. Hence, if multilayer sticking would occur in experimentally accessible situations,these layers could be swept away by the strong flow in the simulation.

In the present MD study we consider Hagen-Poiseuille flow of a Lennard-Jones (LJ) liquid through a cylindrical pore formed also by regularly arranged fixed atoms. Let ϵ and σ be the LJ parameters of the fluid particles. Then the pore wall consists of 16 rings each having 25 equally spaced atoms on a circle with radius 5σ. The rings are places such that the atoms form a triangular lattice on the cylinder; hence, the height of the central cylinder is 17.41σ. For the interaction of the wall with the fluid particles also LJ potentials are assumed with the same σ. Two differently strong solid-fluid interactions, however, are considered. In the weakly attractive case the solid-fluid potential depth parameter ϵ_{SF} is the same as in the fluid, in the strongly attractive case $\epsilon_{SF}=3.5\epsilon$. The factor 3.5 was found by matching the depth of the potential well to that of argon in a smooth carbon pore considered earlier.[6-8] For flow studies the use of structured instead of smooth walls has the advantage that the linear momentum gained by the driving force is dissipated by friction without problems.

The simulations were performed with 915 fluid particles which corresponds to an average reduced density $\langle n\sigma^3\rangle$ of about 0.80. Periodic boundary conditions are assumed in the direction of the pore axis (z axis). Before switching on the driving force the system was equilibrated at a prescribed temperature. At that state the chemical potential can be measured by our modification of the test-particle method.[8] The calculations were performed with vectorized codes on the CYBER 205 computer; technical details have been described elsewhere.[8] The driving force was assumed of gravitational type in the negative z direction with an acceleration $g=0.1\epsilon/m\sigma$ or with the tenfold value.

Hydrodynamic, thermodynamic, and structural quantities were calculated in order to characterize and control the flow. In the following, quantitative results will be reported only for steady-state flows in which case usual intervals for time averaging were applied. Considering the local dependence, we took explicitly account of the radial distance ρ from the pore axis, while the dependence on z and the azimuthal angle was averaged out. The quantities calculated were the total particle flux $\dot{N}$, the local density $n(\rho)=\langle n\rangle_\rho$, the local drift velocity $v_D(\rho)=\langle v_z\rangle_\rho$, and the local kinetic temperatures $T_x(\rho)$, $T_y(\rho)$, and $T_z(\rho)$ with, especially,

$$kT_z(\rho)=m\langle[v_z-v_D(\rho)]^2\rangle_\rho\ .$$

The bracket $\langle\ \rangle_\rho$ denotes averaging in a cylindrical shell

of thickness $\Delta\rho=0.05\sigma$ at ρ. It is convenient to use the reduced quantities $\tilde{\rho}=\rho/\sigma$, $\tilde{n}=n\sigma^3$, $\tilde{T}=kT/\epsilon$, $\tilde{g}=gm\sigma/\epsilon$, $\tilde{v}=v(m/\epsilon)^{1/2}$, and $\tilde{N}=\dot{N}\sigma(m/\epsilon)^{1/2}$ and omit the tilde if no confusion can occur.

A crucial question is the dissipation of the energy or heat produced by the driving force. We tried two different methods both of which resulted in steady-state flows. (a) The velocities were scaled down to keep the local kinetic temperature constant in the entire pore and equal to the initial equilibrium temperature; we call that total-temperature scaling (TTS). (b) The velocities were scaled down to keep the local kinetic temperature constant in the fluid layer closest to the wall and equal to the initial equilibrium temperature; we call that wall-temperature scaling (WTS) and believe that to be the more realistic mechanism for dissipating the produced heat. We are aware of the fact that with WTS we are not working in a rigorously defined mechanical ensemble as would be the case, e.g., in a Nosé-Hoover thermostat. Application of such a thermostat, however, requires an additional free parameter[9] which again would create some arbitrariness in the results.

The parameters of seven simulation runs as well as the resulting particle fluxes are compiled in Table I. The runs were performed in the steady state over 50 000 to 80 000 time steps of duration $\Delta t=0.005\sigma(m/\epsilon)^{1/2}$.

Let us consider first the density and velocity profiles of runs 1 and 2 displayed in Fig. 1. For both systems the temperature is low, the smaller driving force (which on the macroscopic scale is still extremely large) acts, and the heat is dissipated by temperature scaling in the fluid layer closest to the wall (WTS). The difference is in the strength of the wall-fluid interaction which for run 1, corresponds to the carbon-argon interaction while being considerably weaker for run 2. Note that run 2 is rather similar to the pure fluid run in Ref. 3 and comparison of the velocity profiles shows resonable agreement. The most remarkable result, however, is that in run 1 the first two layers at the wall do not flow at all. At that point it seems worth considering the equilibrium state of run 1 in more detail. From previous work for argon in a smooth carbon pore[10] we expect the fluid in the pore to be a stable liquid while the equilibrium bulk fluid outside the pore is a gas with a density considerably less than the dew density. In order to confirm the gaseous state outside we have determined the chemical potential of the fluid in the pore by our modified test-particle method.[8]

TABLE I. Temperature T, acceleration g, wall-fluid interaction ϵ_{SF}/ϵ, and heat-dissipation mechanism (HDM), as well as the resulting particle flux $\dot{N}$ of the simulation runs.

Run	T	g	ϵ_{SF}/ϵ	HDM	$\dot{N}$
1	0.835	0.1	3.5	WTS	1.3
2	0.835	0.1	1.0	WTS	5.7
3	2.0	0.1	3.5	WTS	3.2
4	2.0	0.1	1.0	WTS	7.2
5	0.835	1.0	3.5	WTS	27.2
6	0.835	1.0	3.5	TTS	8.0
7	0.835	0.1	1.0	TTS	2.3

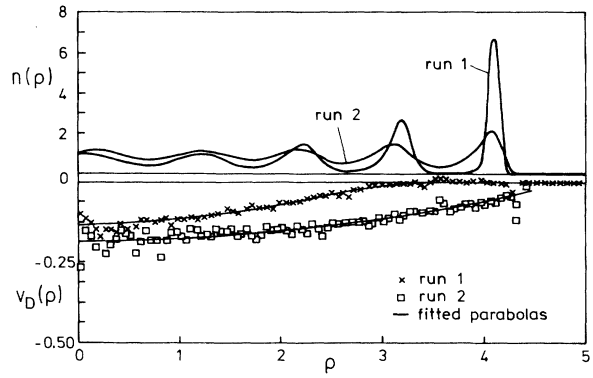

FIG. 1. Density (top) and velocity (bottom) profiles for runs 1 and 2.

The result was $\mu/kT=-6.42$ with a normalization such that for a homogeneous rarefied gas $\mu/kT=\ln\tilde{n}$. As the bulk dew density at $T=0.835$ is obtained by interpolation of Adams[11] results as $n''=0.0077$, the outside gas density for run 1 is found to be about 20% of the dew density. On the other hand, we have analyzed the fluid structure in the pore and found that the molecules in the first adsorbed layer are quite regularly arranged in register with the triangular lattice of the wall atoms. The second layer is also still strongly structured. In going from equilibrium to flow it was already observed by Bitsanis *et al.*[4] that at least the structure perpendicular to the wall does not change very much. Our calculations confirmed that finding. Summarizing, we can say that a fluid being a gas outside a pore can be in a condensed state inside with structured adsorbed layers such that even strong driving forces cannot move these layers. If the wall forces then become weaker, these layers start to flow, which is what happened in run 2. For both runs, the velocity profiles can be fitted by parabolas having, however, zeros R_i at different distances from the pore axis; the ratio R_2/R_1 is approximately 1.5. These parabolas are also shown in Fig. 1. Moreover, looking at Table I we note that the particle flux $\dot{N}$ in run 2 is 5.7 while it is 1.3 in run 1. The ratio is 4.4, which is close to $(R_2/R_1)^4$.

In the next step we wanted to see the effect of the temperature on the flow pattern and considered the same model as in runs 1 and 2 but now at $T=2.0$, a temperature which is about twice the critical temperature in the pore[8] and also higher than the bulk critical temperature. The results in Fig. 2 show that the velocity in the weakly adsorbing pore, run 4, has become a little bigger but otherwise no great change occurred. On the other hand, we notice that now in case of the strongly attractive wall, run 3, only one layer sticks at the wall. The second layer has started to flow. The particle fluxes in Table I reflect once more the described situation.

Then our interest was to study the effect of the driving force. A natural choice would have been to make the driving force more realistic, which means considerably smaller. Then, however, the flow would be hidden in the fluctuations of the simulation. Hence, we went the opposite direction and starting from run 1 we made, in run 5,

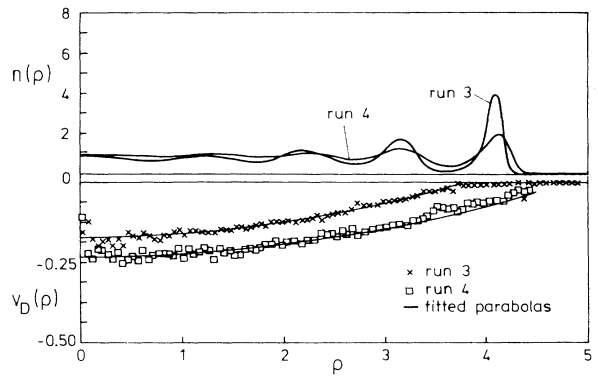

FIG. 2. Density (top) and velocity (bottom) profiles for runs 3 and 4.

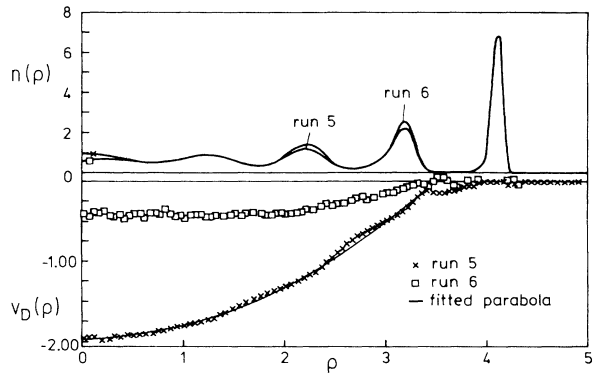

FIG. 3. Density (top) and velocity (bottom) profiles for runs 5 and 6.

the driving force ten times larger. As seen in Fig. 3, the drift velocity is now more than ten times larger in the pore axis and the second layer does not stick anymore at the wall. This confirms our conjecture that sticking layers can be swept away by a sufficiently large driving force. Note that the velocity profile can still be represented by a parabola.

All the above-mentioned simulations were performed with temperature scaling in the fluid layer closest to the wall, the WTS mechanism. In order to see the effect of the different heat dissipation mechanisms, we started from the same model as in run 5 but applied in run 6 the total-temperature scaling (TTS) method. The resulting velocity profile, also displayed in Fig. 3, is completely different from run 5. The velocity in the pore axis is considerably smaller and remains nearly constant up to $\rho=2$. The difference can also be seen from the particle flux $\dot{N}$ in Table I, which decreases by a factor of 3.4. As this is admittedly an extreme situation because of the large driving force, we also used the same model as in run 2 but applied in run 7 TTS scaling. From Table I we learn that even then the particle flux decreases considerably.

To summarize, two essential conclusions may be drawn from this study. First, one must take care in nonequilibrium thermodynamics how to remove the heat. The method preferred by us is WTS, i.e., scaling the temperature in the fluid layer closest to the wall. While this is an ad hoc assumption, we believe, however, that it mimics in some way the effect of the thermostated wall on the fluid. If the heat would have been directly transferred to the wall, some harmonic-oscillator strength would have been needed again to be some arbitrary parameter.

As far as the slip problem is concerned we have found that up to two molecular layers may stick at the wall even at high driving forces, which confirms the recent experimental findings of Chan and Horn.[1] Extrapolating from our results to driving forces of realistic strength, one could imagine that for strong wall forces at low temperature even more layers could be immobilized at the wall. It cannot be excluded that for weaker wall forces also one fluid layer may stick at the wall. It seems to us that the detailed flow behavior near solid boundaries may be strongly affected by the equilibrium structure of the fluid at the wall.

The authors thank Professor H. T. Davis, Professor H. Posch, and Professor W. G. Hoover for helpful discussions and receipt of manuscripts prior to publication. This work was supported by Stiftung Volkswagenwerk im Schwerpunkt "Mathematische und Theoretische Grundlagen in den Ingenieurwissenschaften," AZ., Grant No. I/61 066.

[1]D. Y. C. Chan and R. G. Horn, J. Chem. Phys. **83**, 5311 (1985).
[2]L. Hannon, G. C. Lie, and E. Clementi, Phys. Lett. A **119**, 174 (1986).
[3]J. Koplik, J. R. Banavar, and J. F. Willemsen, Phys. Rev. Lett. **60**, 1282 (1988).
[4]I. Bitsanis, J. J. Magda, M. Tirrell, and H. T. Davis, J. Chem. Phys. **87**, 1733 (1987).
[5]J. Fischer and M. Methfessel, Phys. Rev. A **22**, 2836 (1980).
[6]U. Heinbuch and J. Fischer, in *Proceedings of the Second Conference on Fundamentals of Adsorption, Santa Barbara, 1986,* edited by A. I. Liapis (American Institute of Chemical Engineering, New York, 1987), p. 245.
[7]U. Heinbuch and J. Fischer, Chem. Phys. Lett. **135**, 587 (1987).
[8]U. Heinbuch and J. Fischer, Mol. Simulation **1**, 109 (1987).
[9]H. Posch and W. G. Hoover, Phys. Rev. A **39**, 2175 (1989).
[10]U. Heinbuch and J. Fischer, Chem. Ing. Tech. **60**, 636 (1988).
[11]D. J. Adams, Molec. Phys. **32**, 647 (1976).